

## SVPWM technique for 3-ph 6-switch and 3-ph 4-switch inverters - a comparison

Golkonda Anitha<sup>1</sup>, Kondreddi Krishnaveni<sup>2</sup>, Guduri Yesuratnam<sup>3</sup>

<sup>1</sup>Department of Electrical Engineering, University College of Engineering, Osmania University, Hyderabad, India

<sup>2</sup>Department of Electrical and Electronics Engineering, Chaitanya Bharati Institute of Technology, Hyderabad, India

<sup>3</sup>Department of Electrical Engineering, University College of Engineering, Osmania University, Hyderabad, India

### Article Info

#### Article history:

Received Feb 13, 2024

Revised Jun 30, 2024

Accepted Jul 24, 2024

#### Keywords:

3-ph 4-switch inverter (TPFSI)

3-ph 6-switch inverter (TPSSI)

Clarke's transformation

DC-link voltage

IGBT

SVPWM

### ABSTRACT

A novel 3-phase 4-switch inverter (TPFSI) is described in this study to reduce the inverter's size, complexity, cost, and losses during the conduction and switching process. This TPFSI inverter is based on the principle of similarity of a 3-phase 6-switch inverter (TPSSI) where  $\alpha\beta$  plane is separated into six sectors to form the required reference voltage space vector. It has been demonstrated that TPFSI inverters are more efficient than TPSS inverters while operating with different loads. A mathematical concept for the space vector pulse width modulation (SVPWM) technique has been developed for TPFSI by using Clarke's transformation. In this paper, a TPFSI inverter model is designed to reduce the harmonic content in the output voltage and current responses when connected to different loads. The suggested modulation method enhances the output voltage/current response, resulting in usually balanced waveforms and reduced harmonic distortion. MATLAB/Simulink software is utilized to analyze the output response of both inverters.

*This is an open access article under the [CC BY-SA](https://creativecommons.org/licenses/by-sa/4.0/) license.*



### Corresponding Author:

Golkonda Anitha

Department of Electrical Engineering, University College of Engineering, Osmania University

Hyderabad, India

Email: mahanitha2006@gmail.com

## 1. INTRODUCTION

Solar energy is a crucial renewable source that offers several benefits over non-renewable sources such as fossil fuels and coal. Solar energy generation is both ecologically beneficial and comparatively easy [1]. The inverter, considered the center of any solar energy system, transforms DC to AC and the switches are handled to provide synchronized and balanced AC output waveforms. A transformer is used in conventional inverters to boost the generated voltage to the required voltage. In photo voltaic (PV) applications, transformers are frequently utilized; however, the inverters' efficiency and power density are reduced by these conventional transformers, which also increase the inverters' weight, size, and cost. It is therefore preferable to avoid employing transformers in the inverter [2].

In some cases, cost reduction is an important target for the drive system. However, in the development of research for the inverter topologies to minimize components and reduce the cost and complexity of the system. Hence, the results prove that it is possible to replace a traditional 6-switch inverter with a reduced number of switches (with four switching devices) [3]. The traditional 3-phase 6-switch inverter (TPSSI) is now available in a more affordable form called 3-phase 4-switch inverter (TPFSI) also referred to as the B4 inverter. Several research investigations have been done to expand the application of four-switch inverters, especially in AC electrical machine drive systems [4]-[6]. The TPFSI inverter is composed of two switching legs with four power switches each and one power leg with two serial capacitors as two load phases are taken from two

inverter legs, while the third phase is drawn from a DC-link at the midpoint of two split capacitors, as shown in Figure 1.

The two inverter legs feed phases a and b, while phase c is fed to the central points of capacitors C1 and C2. Significant reductions in switching and conduction losses are achieved by using fewer power switches as compared to the TPSSI. As a result, TPFSI provides greater efficiency than TPSSI. Its drawbacks include an unbalanced output response caused by circulating currents passing in the middle of two capacitors, notwithstanding its benefits. Numerous studies attempted to find a way to remove the distortions in the unbalanced voltage and current responses [7]-[11]. Zhu C *et al.* [7] proposed a compensating voltage vector for the elimination of DC-link voltage offset. Lee *et al.* [8] investigated a control algorithm developed to produce a switching pattern for the SVPWM power inverter J. Kim *et al.* [9] discussed a current distortion compensation technique for unbalanced currents in the motor terminal. Zhou *et al.* [10] discussed a predictive torque control (PTC) scheme for DC-link voltage offset suppression based on the establishment of basic space vectors and modulation techniques. Fadil *et al.* [11] discussed dc-link capacitor voltage imbalance with the DC component from the control reference voltage using low pass filters. Lee *et al.* [12] investigated a simple compensation method that adjusts the switching times considering DC-link voltage ripples. Menon and Jacob [13] proposed a simplified space vector (SV) pulse density modulation scheme without coordinate transformation and sector identification over the SVPWM method. The primary contribution of this paper is to develop a mathematical concept of SVPWM by using Clarke's transformation for cost-effective inverters and to improve DC-link compensation to get balanced output responses. From the above discussion, most of the literature on B4 inverter is relevant to drive systems only.

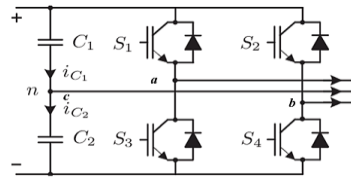


Figure 1. 3-ph 4-switch inverter

## 2. COMPARISON OF MATHEMATICAL CONCEPT OF SVPWM

This paper addresses the modified SVPWM technique for the TPFS inverter based on the principle of similarity of the TPSS inverter where  $\alpha\beta$  plane is divided into 4 space vectors. Among all other PWM techniques, SVPWM is because of its better DC-bus utilization, and simpler digital realization, it differs considerably from all other PWM approaches and increasing trend nowadays which is used mostly for the 3-ph inverters [14]. SVPWM is a vector approach to PWM for 3-phase inverters generating a high voltage, low total harmonic distortion (THD), and generating a sine wave is a sophisticated process [15].

### 2.1. 3-ph 6-switch inverter (TPSSI)

Figure 2 displays the circuit diagram of the TPSSI which consists of six switches (3 with upper-side switches are S1, S3, and S5 and lower-side switches are S4, S6, and S2) operating at  $180^\circ$  conduction mode with the sequence of 561, 612, 123, 234, 345 & 456, and Table 1 displays the corresponding line and voltages with 8 possible switching combinations [100], [110], [010], [011], [001], [101], [111] & [000]. Among the eight switching states, [111] and [000] are null states, and the others are active states. Figure 3 illustrates the block diagram of the SVPWM technique, which is applied to both inverters.

Now the 3-phase system is transformed into a two-phase system by using Clark's transformation as displayed in Figure 4. The 3-phase quantities  $abc$  are shifted by  $120^\circ$  and the  $dq$  axis two-dimensional frame of reference is at  $90^\circ$ . Vectors in the  $d-q$  frame are (1) and (2).

$$\vec{V} = Vd + jVq \quad (1)$$

$$\vec{V} = \frac{2}{3} [Va(t) + a Vb(t) + a^2 Vc(t)] \quad (2)$$

where  $a$  is a unit vector,  $a = 1\angle 120^\circ = e^{j\frac{2\pi}{3}} = -\frac{1}{2} + j\frac{\sqrt{3}}{2}$ ;  $a^2 = 1\angle 240^\circ = e^{j\frac{4\pi}{3}} = -\frac{1}{2} - j\frac{\sqrt{3}}{2}$ . Let the 3-ph sinusoidal voltage components be (3)-(5).

$$Va = Vm \sin \omega t \quad (3)$$

$$V_b = V_m \sin\left(\omega t - \frac{2\pi}{3}\right) \quad (4)$$

$$V_c = V_m \sin\left(\omega t - \frac{4\pi}{3}\right) \quad (5)$$

Where  $V_a$ ,  $V_b$  and  $V_c$  are the phase voltages. These are used to transform a-b-c into d-q frame of reference components by using Clark's Transformation; shown in (6)-(8),

$$\begin{bmatrix} V_d \\ V_q \end{bmatrix} = \frac{2}{3} \begin{bmatrix} 1 & -\frac{1}{2} & -\frac{1}{2} \\ 0 & \frac{\sqrt{3}}{2} & -\frac{\sqrt{3}}{2} \end{bmatrix} \begin{bmatrix} V_a \\ V_b \\ V_c \end{bmatrix} \quad (6)$$

$$|V_{ref}| = \sqrt{V_d^2 + V_q^2} \quad (7)$$

$$\alpha = \tan^{-1}\left(\frac{V_q}{V_d}\right) \quad (8)$$

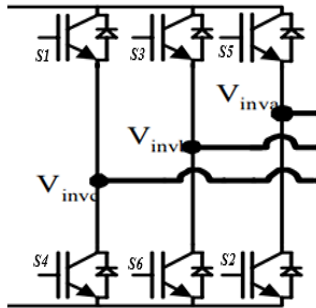


Figure 2. 3-ph 6-switch inverter

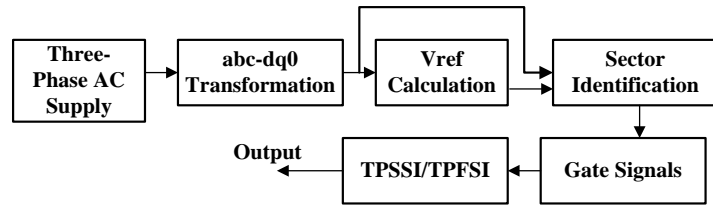


Figure 3. Block diagram of the SVPWM technique

To calculate  $V_{ref}$  at the load, the duty cycle of these switching states and the time of switching states are calculated. This is the basic concept behind the SVPWM Technique. In SVPWM, at any point over the circle, it has a certain value of voltage and angle. Table 1 shows that the space vectors are of the same magnitude but the angle changes over the circle by an angle of  $60^\circ$ .  $V_{ref}$  is constructed by the combination of  $V_1$ ,  $V_2$  &  $V_0$  whatever area must be covered by reference vector from (9)-(11).

$$\int_0^{T_z} V_{ref} dt = \int_0^{T_1} V_1 dt + \int_{T_1}^{T_1+T_2} V_2 dt + \int_{T_1+T_2}^{T_1+T_2+T_0} V_0 dt \quad (9)$$

$$V_{ref} T_z = V_1 T_1 + V_2 T_2 + V_0 T_0 \quad (10)$$

$$V_{ref} = V_1 D_1 + V_2 D_2 + V_0 D_0 \quad (11)$$

Table 1. Line and phase voltages, switching vectors, and space vectors

Voltage vectors	Switching states			Line-Neutral Voltages			Line-Line voltages			On state switch	Space vector
	a	b	c	$U_{an}$	$U_{bn}$	$U_{cn}$	$U_{ab}$	$U_{bc}$	$U_{ca}$		
$V_0$	0	0	0	0	0	0	0	0	0	S1, S3, S5	0
$V_1$	1	0	0	$2/3$	$-1/3$	$-1/3$	1	0	-1	S1, S6, S2	$\frac{2}{3} \angle 0^\circ$
$V_2$	1	1	0	$1/3$	$1/3$	$-2/3$	0	1	-1	S1, S3, S2	$\frac{2}{3} \angle 60^\circ$
$V_3$	0	1	0	$-1/3$	$2/3$	$-1/3$	-1	1	0	S4, S3, S2	$\frac{2}{3} \angle 120^\circ$
$V_4$	0	1	1	$-2/3$	$1/3$	$1/3$	-1	0	1	S4, S3, S5	$\frac{2}{3} \angle 180^\circ$
$V_5$	0	0	1	$-1/3$	$-1/3$	$2/3$	0	-1	1	S4, S6, S5	$\frac{2}{3} \angle 240^\circ$
$V_6$	1	0	1	$1/3$	$-2/3$	$1/3$	1	-1	0	S1, S6, S5	$\frac{2}{3} \angle 300^\circ$
$V_7$	1	1	1	0	0	0	0	0	0	S4, S6, S2	0

In (10) can be written in the d-axis and q-axis components as shown in (12).

$$V_{ref} \begin{bmatrix} \cos\alpha \\ \sin\alpha \end{bmatrix} T_z = \frac{2}{3} V_s \begin{bmatrix} \cos 0^\circ \\ \sin 0^\circ \end{bmatrix} T_1 + \frac{2}{3} V_s \begin{bmatrix} \cos \frac{\pi}{3} \\ \sin \frac{\pi}{3} \end{bmatrix} T_2 \quad (12)$$

By comparing d and q-axis quantities from (12), T1 and T2 can be calculated from (13)-(18).

$$V_{ref} \sin\alpha T_z = \frac{2}{3} V_s \sin 0^\circ T_1 + \frac{2}{3} V_s \sin \frac{\pi}{3} T_2 \quad (13)$$

$$T_2 = a \frac{\sin\alpha}{\sin\pi/3} T_z \quad (14)$$

Where  $a = \frac{\frac{2}{3} V_{ref}}{V_s}$  = modulation index must be less than 1. Now comparing d-axis quantities

$$V_{ref} \cos\alpha T_z = \frac{2}{3} V_s \cos 0^\circ T_1 + \frac{2}{3} V_s \cos \frac{\pi}{3} T_2 \quad (15)$$

$$T_1 = \frac{V_{ref} \cos\alpha T_z}{\frac{2}{3} V_s} - \frac{\frac{2}{3} V_s \cos\pi/3 T_2}{\frac{2}{3} V_s} \quad (16)$$

$$T_1 = a \cos\alpha T_z - \cos \frac{\pi}{3} T_2 \quad (17)$$

Substituting (14) in (17), we get (18).

$$T_1 = a T_z \frac{\sin(\frac{\pi}{3}-\alpha)}{\sin\pi/3} \quad (18)$$

Now calculate the time duration for the null vector as shown in (19).

$$T_0 = T_z - T_1 - T_2 \quad (19)$$

The (14), (18), and (19) are the time durations (T1, T2, and T0) for adjacent switching space vectors V1 & V2 and two null vectors V0 & V7. For n vectors, the time durations for all the sectors are calculated as (20)-(22).

$$T_1 = a \frac{T_z \sin(\frac{n\pi}{3}-\alpha)}{\sin\pi/3} \quad (20)$$

$$T_2 = a \frac{T_z \sin[\alpha-(n-1)\pi]}{\sin\pi/3} \quad (21)$$

$$T_0 = T_z - T_1 - T_2 \quad (22)$$

Where  $T_z$  denotes the switching time. Next determining the switching time of the upper and lower switches as shown in Table 2.

## 2.2. 3-ph 4-switch inverter (TPFSI)

Different controllers were applied for the generation of reference signals to produce the PWM signals for the 4-switch 3-ph inverter. The modulation technique of the 3-ph 4-switch is quite different which was discussed in [16]-[18]. Phan Quoc Dzung *et al.* [19] modified an SVPWM algorithm for FSTP based on the 6-switch 3-ph inverters is proposed. Since one phase is constantly connected to the middle of the two DC-link capacitors in the four-switch converter. Hence current flows even at the zero vector. Furthermore, only the remaining current from the other two phases passes through the phase connected to the midpoint of the two DC-link capacitors when the switching states are (0, 1) and (1, 0) [20]. The switching states S1, S2, S3, and S4 are used to represent the binary variables 1 and 0, when the upper switch is closed, the set of switches is set to "1". When the upper switch is open, the set of switches is set to "0". The switches in one inverter branch are alternated. So that:  $S1+S2=1$ ;  $S3+S4=1$ . The SVPWM techniques for the 4-switch inverter are based on the formation of the reference vector of the  $\alpha\beta$  plane which is divided into 4 sectors [21], [22] as shown in Figure 4. The active vectors and their durations in a sampling interval are chosen and calculated for these

sectors V1, V2, V3, and V4 based on the location of  $V_{ref}$  discussed in papers [23]-[26]. Figure 5 displays the SV diagram of the TPFS inverter and Figure 6 shows the SVPWM approach to the 3-ph 6-switch inverter.

Table 2. Determining the switching time of the upper and lower switch with switching intervals

Sector	Upper switches	Lower switches	Range of angle
1	$S1=T1+T2+T_o/2$ $S3=T2+T_o/2$ $S5= T_o/2$	$S4= T_o/2$ $S6=T1+T_o/2$ $S2=T1+T2+T_o/2$	$0^\circ < \alpha < 60^\circ$
2	$S1= T1+T_o/2$ $S3=T1+T2+T_o/2$ $S5= T_o/2$	$S4= T2+T_o/2$ $S6=T_o/2$ $S2=T1+T2+T_o/2$	$60^\circ < \alpha < 120^\circ$
3	$S1= T_o/2$ $S3= T1+T2+T_o/2$ $S5= T2+T_o/2$	$S4= T1+T2+T_o/2$ $S6= T_o/2$ $S2= T1+T_o/2$	$120^\circ < \alpha < 180^\circ$
4	$S1= T_o/2$ $S3= T1+T_o/2$ $S5= T1+T2+T_o/2$	$S4= T1+T2+T_o/2$ $S6= T2+T_o/2$ $S2= T_o/2$	$180^\circ < \alpha < 240^\circ$
5	$S1= T2+T_o/2$ $S3= T_o/2$ $S5= T1+T2+T_o/2$	$S4= T1+T_o/2$ $S6= T1+T2+T_o/2$ $S2= T_o/2$	$240^\circ < \alpha < 300^\circ$
6	$S1= T1+T2+T_o/2$ $S3= T_o/2$ $S5= T1+T_o/2$	$S4= T_o/2$ $S6= T1+T2+T_o/2$ $S2= T2+T_o/2$	$300^\circ < \alpha < 360^\circ$

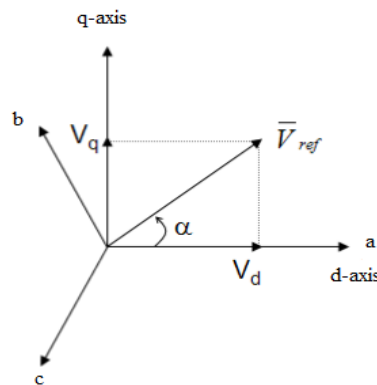


Figure 4. The relationship between (abc) and (dq) reference frame

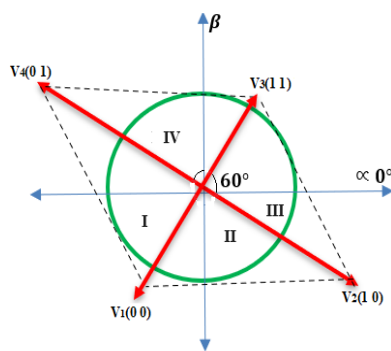


Figure 5. Space vector diagram for TPFSI

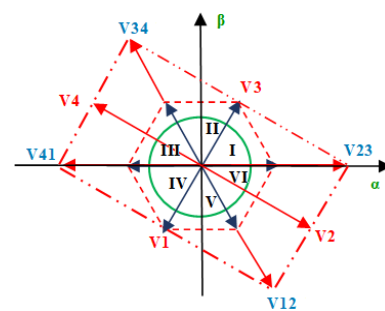


Figure 6. SVPWM approach for TPFSI and TPSSI

After calculating vectors that divide the plane into 4 sectors each sector is conducting for of  $90^\circ$ .  $V_{ref}$  is generated by two adjacent non-zero vectors. The sectors and their range for a 3-ph 4-switch inverter are given in Table 3 which shows the calculation of the switching time of each switch. Thus, calculating the switching time of each sector, at  $90^\circ$  similar to TPSSI as shown in Table 4. The Switching diagram for each sector is shown in Figure 7 and in the case of SSTPI magnitude remains same by an angle  $60^\circ$ .

Table 3. Switching vectors, line-neutral voltages, line-line voltages

Voltage vectors	Switching vectors		Line-neutral voltage			Line-line voltages			Space vector	Range of angle
	a	b	$V_{an}$	$V_{bn}$	$V_{cn}$	$V_{ab}$	$V_{bc}$	$V_{ca}$		
$V_1$	0	0	-1/3	-1/3	2/3	0	-1	1	$\frac{2}{3}\angle -120^\circ$	$-120^\circ < \alpha < -30^\circ$
$V_2$	1	0	1	-1	0	2	-1	-1	$\frac{2}{3}\angle -30^\circ$	$-30^\circ < \alpha < 60^\circ$
$V_3$	1	1	1/3	1/3	-2/3	0	1	-1	$\frac{2}{3}\angle 60^\circ$	$60^\circ < \alpha < 150^\circ$
$V_4$	0	1	-1	1	0	-2	1	1	$\frac{2}{3}\angle 150^\circ$	$150^\circ < \alpha < -120^\circ$

Table 4. Switching time for each sector

Sectors	Switching time	Upper switch	Lower switch
Sector 1	$T1 = \frac{3V_{ref}\cos\alpha T_z}{2V_s}$	$S1 = T2 + T_o/2$	$S2 = T1 + T_o/2$
	$T2 = \frac{\sqrt{3}V_{ref}\sin\alpha T_z}{2V_s}$	$S3 = T_o/2$	$S4 = T1 + T2 + T_o/2$
	$T_o = T_z - (T1 + T2)$		
Sector 2	$T2 = \frac{\sqrt{3}V_{ref}\sin\alpha T_z}{2V_s}$	$S1 = T1 + T2 + T_o/2$	$S2 = T_o/2$
	$T3 = \frac{-3V_{ref}\cos\alpha T_z}{2V_s}$	$S3 = T2 + T_o/2$	$S4 = T1 + T_o/2$
	$T_o = T_z - (T1 + T2)$		
Sector 3	$T3 = \frac{-3V_{ref}\cos\alpha T_z}{2V_s}$	$S1 = T1 + T_o/2$	$S2 = T2 + T_o/2$
	$T4 = \frac{-\sqrt{3}V_{ref}\sin\alpha T_z}{2V_s}$	$S3 = T1 + T2 + T_o/2$	$S4 = T_o/2$
	$T_o = T_z - (T1 + T2)$		
Sector 4	$T2 = \frac{\sqrt{3}V_{ref}\sin\alpha T_z}{2V_s}$	$S1 = T_o/2$	$S2 = T1 + T2 + T_o/2$
	$T1 = \frac{3V_{ref}\cos\alpha T_z}{2V_s}$	$S3 = T1 + T_o/2$	$S4 = T2 + T_o/2$
	$T_o = T_z - (T1 + T2)$		

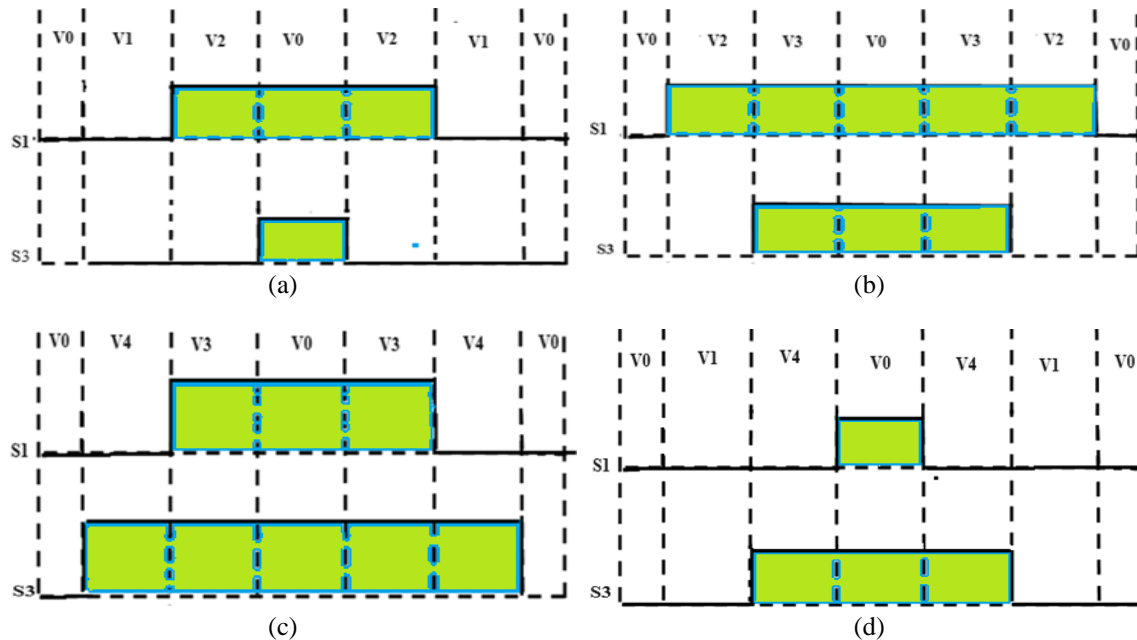


Figure 7. Switching diagram of each (a) sector I, (b) sector II, (c) sector III, and (d) sector IV

### 3. RESULTS AND ANALYSIS

MATLAB/Simulink software was utilized to do the simulations of the basic operation of the SVPWM technique for a 3-ph 4-switch inverter. Based on the modeling and observations discussed above, the proposed

converter and its theory of operation are evaluated. Figures 8(a) and 8(b) display the sector and angle for TPSS and TPFS inverters respectively. Figures 9(a) and 9(b) indicate the Phase and Line voltages of the six-switch inverter, and TPFS inverter which are unbalanced due to the circulating currents without the filter design. Figure 10(a) shows the time of switching sequence Ta1 and Ta2 of the TPFS inverter according to sectors for one cycle of the output voltage, and Figure 10(b) shows the gate signals for switches S1 and S3 which are complementary to switches S2 and S4. The model parameters for both inverters are input voltage = 200 V; Dc-link capacitors,  $C1 = C2 = 1000 \mu\text{F}$ ; filter capacitor,  $C_f = 100 \mu\text{F}$ ; filter inductor,  $L_f = 1 \text{ mH}$ ; load resistance =  $100 \Omega$  respectively.

Figure 9(b) makes it clear that the circulating currents through the capacitors are the cause of the unbalanced output response of voltage. This result therefore confirms that the SVPWM technique that was described above has been implemented correctly in suppressing the effect of the voltage unbalance issue on the output line voltage and current. When a resistive load is coupled to a 3-ph 6-switch and 4-switch inverter the output response is depicted in Figures 11(a) and 11(b). It has been noted that the 3-ph 4-switch inverter output voltage and current response are balanced shown in Figure 11(b). The output voltage and current response of the 3-ph 6-switch inverter when connected to R-load are displayed in Figure 11(a). This leads to the conclusion that the 3-ph 4-switch inverter can successfully replace the 3-ph 6-switch inverter. When this system is connected to the grid the output response is unbalanced and the injected powers (active and reactive) are oscillating. The main problem with a four-switch inverter is an unbalanced response at the grid side. Different control techniques are used in grid-connected PV systems for better results to get a balanced output voltage/current response.

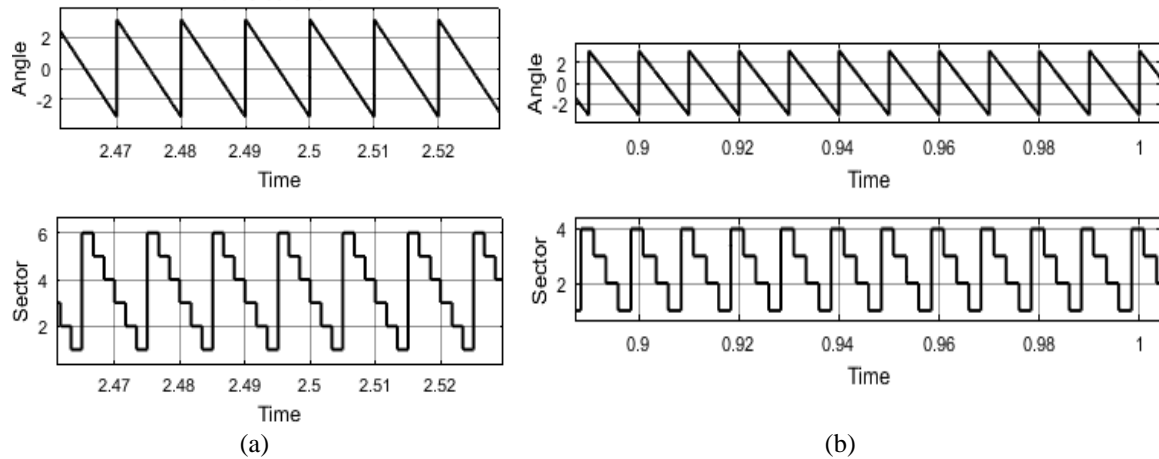


Figure 8. Determination of sector and angle for (a) TPSS inverter and (b) TPFS inverter

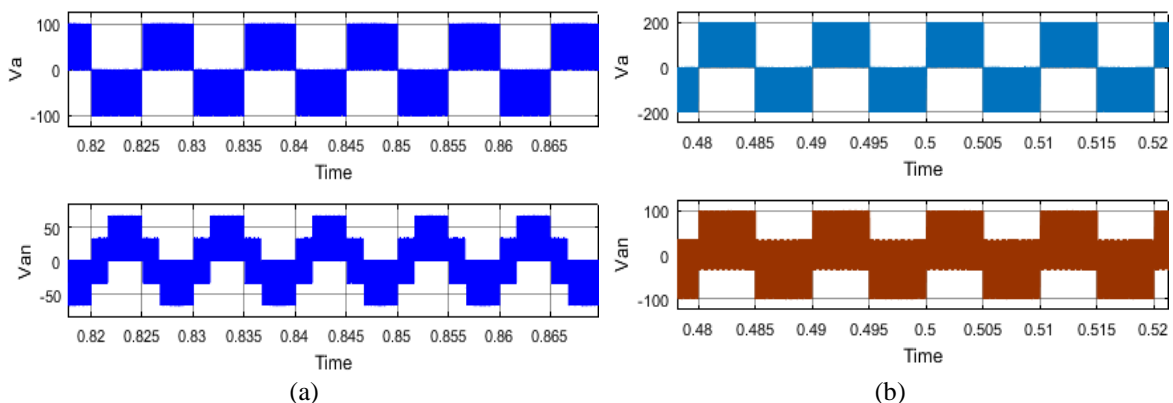


Figure 9. Phase voltages and line voltages of phase 'a' for (a) the TPSS inverter and (b) the TPFS inverter

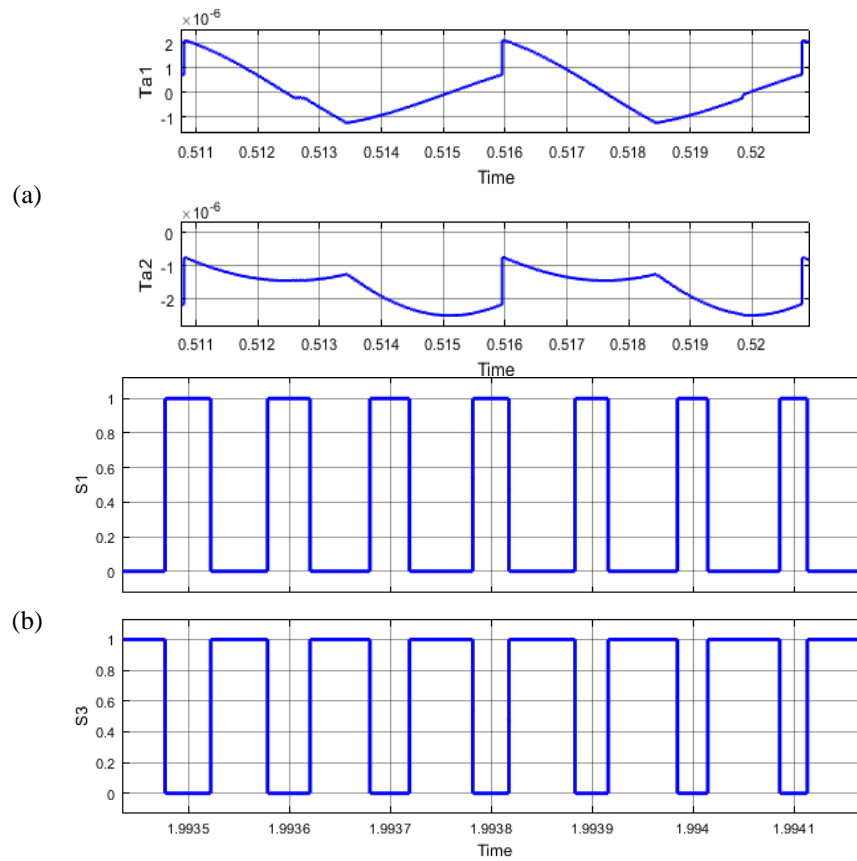


Figure 10. Waveforms of the TPFS inverter for (a) switching times  $T_{a1}$  and  $T_{a2}$  according to sectors for one cycle of the output voltage and (b) gate signals for  $S_1$  and  $S_3$

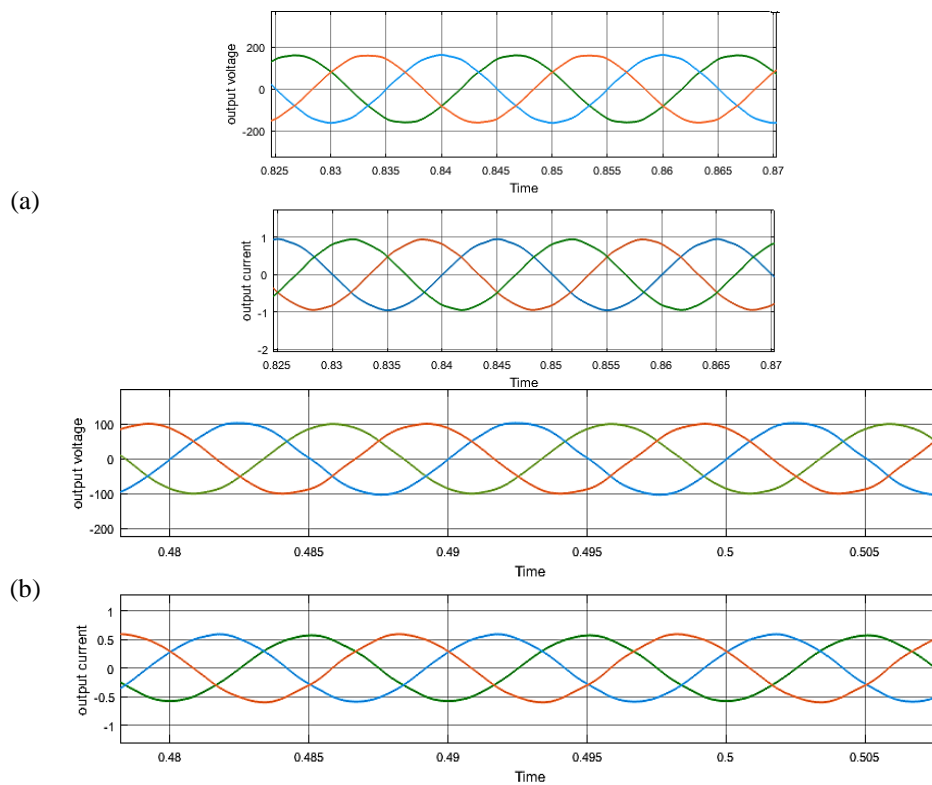


Figure 11. Output voltages and current waveforms for (a) TPSS inverter and (b) TPFS inverter



#### 4. CONCLUSION

This paper compares the SVPWM Technique for two types of inverters: the 3ph 6-switch Inverter (TPSSI) and the 3ph 4-switch Inverter (TPFSI). Using Clarke's transformation, the  $\alpha\beta$  plane is divided into six sectors for TPSSI and four vectors for TPFSI. These sectors provide the necessary reference voltage for space vectors. After conducting a comparison investigation, it was found that in applications where cost is essential, it is possible to replace the 3ph 6-switch inverter with a 3ph 4-switch inverter. The reason for this is that the 3ph 4-switch inverter has a reduced number of components, making it less expensive than the 3ph 6-switch inverter. Most of the literature on B4 inverter is relevant to drive systems only. Additionally, minimizing the switching and conduction loss can increase the overall efficiency of the system. The effect of the capacitor's voltage imbalance issue on the inverter output voltage and current has been solved with the use of an efficient space vector modulation approach by using a better control technique for further work and it is studied for grid-connected inverters. Mathematical calculations are derived for both inverters, and the output response of voltage/current is plotted. MATLAB/Simulink models for both inverters are simulated and observed.

#### ACKNOWLEDGEMENTS

The authors acknowledge the Department of Electrical and Electronics Engineering, Chaitanya Bharati Institute of Technology, Hyderabad, India, and the Department of Electrical Engineering, UCE, Osmania University, Hyderabad, India for providing the necessary facilities which includes a licensed version of MATLAB software.




#### REFERENCES

- [1] M. Hafner and S. Tagliapietra, "The global energy transition: A review of the existing literature," *Lecture Notes in Energy*, vol. 73, pp. 1–24, 2020, doi: 10.1007/978-3-030-39066-2\_1.
- [2] M. N. H. Khan, M. Forouzesh, Y. P. Siwakoti, L. Li, T. Kerekes, and F. Blaabjerg, "Transformerless Inverter Topologies for Single-Phase Photovoltaic Systems: A Comparative Review," *IEEE Journal of Emerging and Selected Topics in Power Electronics*, vol. 8, no. 1, pp. 805–835, 2020, doi: 10.1109/JESTPE.2019.2908672.
- [3] J. D. Van Wyk and H. W. Van Der Broeck, "A Comparative Investigation of a Three-Phase Induction Machine Drive with a Component Minimized Voltage-Fed Inverter under Different Control Options," *IEEE Transactions on Industry Applications*, vol. IA-20, no. 2, pp. 309–320, 1984, doi: 10.1109/TIA.1984.4504413.
- [4] J. Su and D. Sun, "Simplified MPCC for four-switch three-phase inverter-fed PMSM," *Electronics Letters*, vol. 53, no. 16, pp. 1108–1109, 2017, doi: 10.1049/el.2017.1839.
- [5] F. Blaabjerg, S. Freysson, H. H. Hansen, and S. Hansen, "A new optimized space-vector modulation strategy for a component-minimized voltage source inverter," *IEEE Transactions on Power Electronics*, vol. 12, no. 4, pp. 704–714, 1997, doi: 10.1109/63.602566.
- [6] M. B. de Rossiter Corrêa, C. B. Jacobina, E. R. C. da Silva, and A. M. N. Lima, "A general PWM strategy for four-switch three-phase inverters," *IEEE Transactions on Power Electronics*, vol. 21, no. 6, pp. 1618–1627, 2006, doi: 10.1109/TPEL.2006.882964.
- [7] C. Zhu, Z. Zeng, and R. Zhao, "Adaptive suppression method for DC-link voltage offset in three-phase four-switch inverter-fed PMSM drives," *Electronics Letters*, vol. 52, no. 17, pp. 1442–1444, 2016, doi: 10.1049/el.2016.2048.
- [8] H. H. Lee, P. Q. Dzung, L. M. Phuong, and L. D. Khoa, "A new design for four switch three phase inverter based on FPGA for induction motor control," in *TENCON 2009 - 2009 IEEE Region 10 Conference*, Nov. 2009, pp. 1–6, doi: 10.1109/TENCON.2009.5396099.
- [9] J. Kim, J. Hong, and K. Nam, "A current distortion compensation scheme for four-switch inverters," *IEEE Transactions on Power Electronics*, vol. 24, no. 4, pp. 1032–1040, 2009, doi: 10.1109/TPEL.2008.2011552.
- [10] D. Zhou, J. Zhao, and Y. Liu, "Predictive torque control scheme for three-phase four-switch inverter-fed induction motor drives with DC-link voltages offset suppression," *IEEE Transactions on Power Electronics*, vol. 30, no. 6, pp. 3309–3318, 2015, doi: 10.1109/TPEL.2014.2338395.
- [11] H. Fadil, D. Yousfi, M. L. Elhafyani, Y. A. Driss, and A. R. Nasrudin, "Four-switch three-phase PMSM converter with output voltage balance and DC-link voltage offset suppression," in *2016 International Conference on Electrical Sciences and Technologies in Maghreb (CISTEM)*, Oct. 2016, vol. 8, no. 1, pp. 1–7, doi: 10.1109/CISTEM.2016.8066794.
- [12] D. M. Lee, J. B. Park, and H. A. Toliyat, "A simple current ripple reduction method for B4 inverters," *Journal of Electrical Engineering and Technology*, vol. 8, no. 5, pp. 1062–1069, 2013, doi: 10.5370/JEET.2013.8.5.1062.
- [13] M. A. Menon and B. Jacob, "A Simplified Space Vector Pulse Density Modulation Scheme Without Coordinate Transformation and Sector Identification," *IEEE Transactions on Industrial Electronics*, vol. 69, no. 5, pp. 4431–4439, 2022, doi: 10.1109/TIE.2021.3080201.
- [14] T. Murali Krishna, K. Krishna Veni, G. Suresh Babu, D. Sushma, and C. Harish, "Performance evaluation of induction motor for unipolar and bipolar pulse width modulation techniques," *International Journal of Innovative Technology and Exploring Engineering*, vol. 8, no. 10, pp. 3626–3629, 2019, doi: 10.35940/ijitee.J9793.0881019.
- [15] H. Zhang, "A Simplified Space Vector PWM Algorithm for Four-Switch Three-phase Inverters," 2021, doi: 10.1109/PEDG51384.2021.9494166.
- [16] K. Sreeram, "Design of Fuzzy Logic Controller for Speed Control of Sensorless BLDC Motor Drive," in *2018 International Conference on Control, Power, Communication and Computing Technologies, ICCPCT 2018*, 2018, pp. 18–24, doi: 10.1109/ICPCT.2018.8574280.
- [17] H. Zhang, "Imbalance Compensation for SVPWM-Controlled Four-switch Three-phase Inverters," in *2023 IEEE Green Technologies Conference (GreenTech)*, Apr. 2023, pp. 95–100, doi: 10.1109/GreenTech56823.2023.10173831.




- [18] M. S. Zaky and M. K. Metwaly, "A Performance Investigation of a Four-Switch Three-Phase Inverter-Fed im Drives at Low Speeds Using Fuzzy Logic and PI Controllers," *IEEE Transactions on Power Electronics*, vol. 32, no. 5, pp. 3741–3753, 2017, doi: 10.1109/TPEL.2016.2583660.
- [19] P. Q. Dzung, L. M. Phuong, P. Q. Vinh, N. M. Hoang, and T. C. Binh, "New space vector control approach for four switch three phase inverter (FSTPI)," in *Proceedings of the International Conference on Power Electronics and Drive Systems*, 2007, pp. 1002–1008, doi: 10.1109/PEDS.2007.4487826.
- [20] C. T. Lin, C. W. Hung, and C. W. Liu, "Position sensorless control for four-switch three-phase brushless DC motor drives," *IEEE Transactions on Power Electronics*, vol. 23, no. 1, pp. 438–444, 2008, doi: 10.1109/TPEL.2007.911782.
- [21] P. Q. Dzung, L. M. Phuong, and P. Q. Vinh, "The development of artificial neural network space vector PWM for four-switch three-phase inverter," in *Proceedings of the International Conference on Power Electronics and Drive Systems*, 2007, pp. 1009–1014, doi: 10.1109/PEDS.2007.4487827.
- [22] P. Q. Dzung, L. M. Phuong, H. H. Lee, B. N. Thang, and L. D. Khoa, "A new FPGA implementation of four- switch three- phase inverter," in *Proceedings of the International Conference on Power Electronics and Drive Systems*, Nov. 2009, pp. 882–887, doi: 10.1109/PEDS.2009.5385825.
- [23] Z. Zeng, C. Zhu, X. Jin, W. Shi, and R. Zhao, "Hybrid Space Vector Modulation Strategy for Torque Ripple Minimization in Three-Phase Four-Switch Inverter-Fed PMSM Drives," *IEEE Transactions on Industrial Electronics*, vol. 64, no. 3, pp. 2122–2134, 2017, doi: 10.1109/TIE.2016.2625768.
- [24] C. B. Jacobina, E. R. C. da Silva, A. M. N. Lima, and R. L. A. Ribeiro, "Vector and scalar control of a four switch three phase inverter," in *Conference Record - IAS Annual Meeting (IEEE Industry Applications Society)*, 1995, vol. 3, pp. 2422–2429, doi: 10.1109/ias.1995.530611.
- [25] W. Wang, A. Luo, X. Xu, L. Fang, T. M. Chau, and Z. Li, "Space vector pulse-width modulation algorithm and DC-side voltage control strategy of three-phase four-switch active power filters," *IET Power Electronics*, vol. 6, no. 1, pp. 125–135, 2013, doi: 10.1049/iet-pel.2012.0391.
- [26] M. B. R. Correa, C. B. Jacobina, A. M. N. Lima, and E. R. C. Da Silva, "A new approach to generate PWM patterns for four-switch three-phase inverters," in *30th Annual IEEE Power Electronics Specialists Conference. Record. (Cat. No.99CH36321)*, vol. 2, pp. 941–946, doi: 10.1109/PESC.1999.785624.

## BIOGRAPHIES OF AUTHORS






**Golkonda Anitha**    received her B.Tech. in Electrical and Electronics Engineering from the JNTU, Hyderabad, India in 2004 and M.Tech. from JNTU, Hyderabad, India in Power Electronics in 2011. She is currently a Ph.D. student at the University College of Engineering, Osmania University, Hyderabad, India who is doing work related to renewable energy sources of power converters and modulation techniques. She can be contacted at email: mahanitha2006@gmail.com.



**Kondreddi Krishnaveni**    completed her B. Tech from Nagarjuna University in 1992, M.S (DLPD) from BITS, Pilani in 1996, and M.Tech from JNTU, Hyderabad, India in 2002. She is awarded a Ph.D. in Electrical Engineering in the area of Flexible AC Transmission Systems from JNTU, Hyderabad in April 2009. Currently, she is working as a professor in the EEE Department of CBIT(A), Hyderabad. Her research interests include power electronics, FACTS, and applications of power electronics to renewable energy systems. She can be contacted at email: krishnaveni\_eee@cbit.ac.in.



**Guduri Yesuratnam**    completed his B.Tech. from JNTU, Hyderabad, India in 1995 and M. Tech in Power Systems Engineering, Regional Engineering College, Warangal, India in 1997. He was awarded a Ph.D. in Electrical Engineering from the Indian Institute of Science, Bangalore in 2007. Currently, he is working as a Sr. Professor in the Department of Electrical Engineering, at Osmania University, Hyderabad. His research interests include computer aided power system analysis, reactive power optimization, power system security, voltage stability, AI applications in power systems, and gas insulated substations. He is serving as a peer reviewer of international journals. Throughout his career, he has supervised Ph.D. students as well as published many papers in IEEE and international conference proceedings and journals. He can be contacted at email: ratnamgy2003@gmail.com.